

First Synthesis and Characterisation of CH₄@C₆₀

Sally Bloodworth,^[a] Gabriela Sotinova,^[a] Shamim Alom,^[a] Sara Vidal,^[a] George R. Bacanu,^[a] Stuart J. Elliott,^[a,b] Mark E. Light,^[a] Julie M. Herniman,^[a] G. John Langley,^[a] Malcolm H. Levitt,^[a] and Richard J. Whitby^{*[a]}

Abstract: The endohedral fullerene CH₄@C₆₀, in which each C₆₀ fullerene cage encapsulates a single methane molecule, has been synthesised for the first time. CH₄ is the largest molecule, with the greatest number of atoms, to have been encapsulated in C₆₀ to date. The key orifice contraction step, a photochemical desulfinylation of an open fullerene, was successfully completed, even though it is significantly inhibited by the presence of the endohedral molecule. The ¹³C NMR resonance for the cage nuclei in CH₄@C₆₀ is deshielded by $\Delta\delta = +0.52$ ppm relative to C₆₀. The crystal structure of the nickel(II) octaethylporphyrin / benzene solvate shows no significant distortion of the carbon cage, relative to the C₆₀ analogue, and shows the methane hydrogens as a shell of electron density around the central carbon, indicative of the quantum nature of the methane, existing in a set of quantised rotational-translational states at 100 K. The ¹H and ¹³C spin-lattice relaxation times (*T*₁) for endohedral methane have been measured. The ¹H *T*₁ values are similar to those observed in the gas phase, also indicating that methane is freely rotating inside the C₆₀ cage. The ¹H relaxation rate constant *T*₁⁻¹ increases with increasing temperature and suggests a significant spin-rotation contribution to the relaxation. The successful synthesis of CH₄@C₆₀ opens a route to endofullerenes incorporating larger guest molecules than those encapsulated previously.

Soon after the discovery of C₆₀ in 1985,^[1] came recognition that its approximately spherical 3.7 Å diameter cavity provides a unique environment in which to isolate single atoms.^[2] Since then endohedral fullerenes, *i.e.* compounds denoted A@C₆₀ in which molecules or atoms are enclosed within the fullerene cage, have been the focus of substantial experimental and theoretical efforts.^[3–5] Endohedral fullerenes may be synthesised by forming the fullerene in the presence of the endohedral species (particularly successful for metallofullerenes),^[3,5] by high temperature and pressure treatment of the fullerene with the endohedral species (inert gas@C₆₀),^[6,7] or by ion bombardment of the fullerene (N@C₆₀),^[8] but all give very low incorporation and

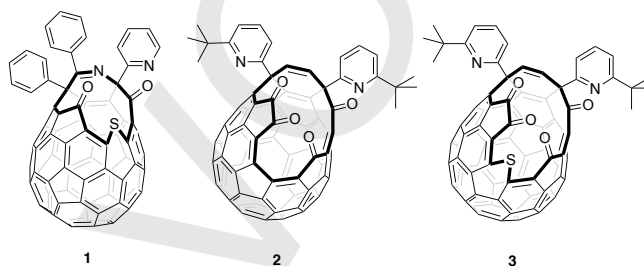


Figure 1. Open-cage fullerenes. Preparation of H₂@C₆₀ from **1**, and of H₂O@C₆₀ and HF@C₆₀ from **2**, is known; as are a series of open-cage derivatives A@**3**.

require extensive purification. Furthermore, these methods are not applicable to the incorporation of small organic molecules.

The macroscopic-scale preparation of endohedral fullerenes by multi-step 'molecular surgery'^[9–12] involves chemically opening an orifice in the fullerene, of a size suitable to allow entry of the single molecule. Suturing of this orifice to restore the pristine carbon cage was pioneered by Komatsu^[13,14] and Murata^[15] who reported the first syntheses of H₂@C₆₀ and H₂O@C₆₀ following insertion of H₂ or H₂O under high-pressure, into open-cage fullerenes **1** and **2** respectively. Optimised procedures for the synthesis of H₂@C₆₀ and H₂O@C₆₀ have subsequently been reported by ourselves,^[16] based on Murata's open-cage C₆₀ derivative **2**, and also applied to the synthesis of HF@C₆₀.^[17,18]

The macroscopic quantities of endohedral fullerenes provided by molecular surgery have allowed detailed investigation of physical properties, including by neutron scattering, infrared spectroscopy and NMR spectroscopy.^[19] These methods have shown that, as a result of the inert and highly symmetrical environment of the cavity, an entrapped molecule behaves much as would be expected in the very low-pressure gas state,^[17,19–23] displaying free rotation at cryogenic temperatures.^[19–24]

The 16-membered orifice of **2** is too small to allow entry of bigger guests, but these can be accommodated by the larger (17-membered) opening of fullerene **3**.^[25] Insertion of N₂ and CO₂,^[26] CH₃OH and H₂CO,^[27] CH₄ and NH₃,^[28] NO^[29] and O₂,^[30] into **3** have all been recently described, but a procedure for suturing the opening of A@**3** to give A@C₆₀ has not yet been reported. In this article, we describe successful closure of A@**3** to give A@C₆₀ for the first time.

The endohedral fullerenes H₂@C₆₀ and H₂O@C₆₀ are exceptional platforms for the study of nuclear spin isomerism,^[24,31–33] in which only certain combinations of nuclear spin states and molecular rotational states are allowed by the Pauli principle. We are particularly interested in CH₄@C₆₀, since spin isomerism is also

[a] Dr. S. Bloodworth, Miss. G. Sotinova, Mr. S. Alom, Dr. S. Vidal, Mr. G. R. Bacanu, Dr. S. J. Elliott, Dr. M. E. Light, Miss. J. M. Herniman, Prof. G. J. Langley, Prof. M. H. Levitt, Prof. R. J. Whitby*
Chemistry, Faculty of Engineering and Physical Sciences
University of Southampton
Southampton, SO17 1BJ (UK)
E-mail: rjw1@soton.ac.uk

[b] Dr. S. J. Elliott, current address:
Centre de Résonance Magnétique Nucléaire à Très Hauts Champs,
FRE 2034 Université de Lyon, CNRS,
Université Claude Bernard Lyon 1, ENS de Lyon, 5 Rue de la Doua,
69100 Villeurbanne (France)

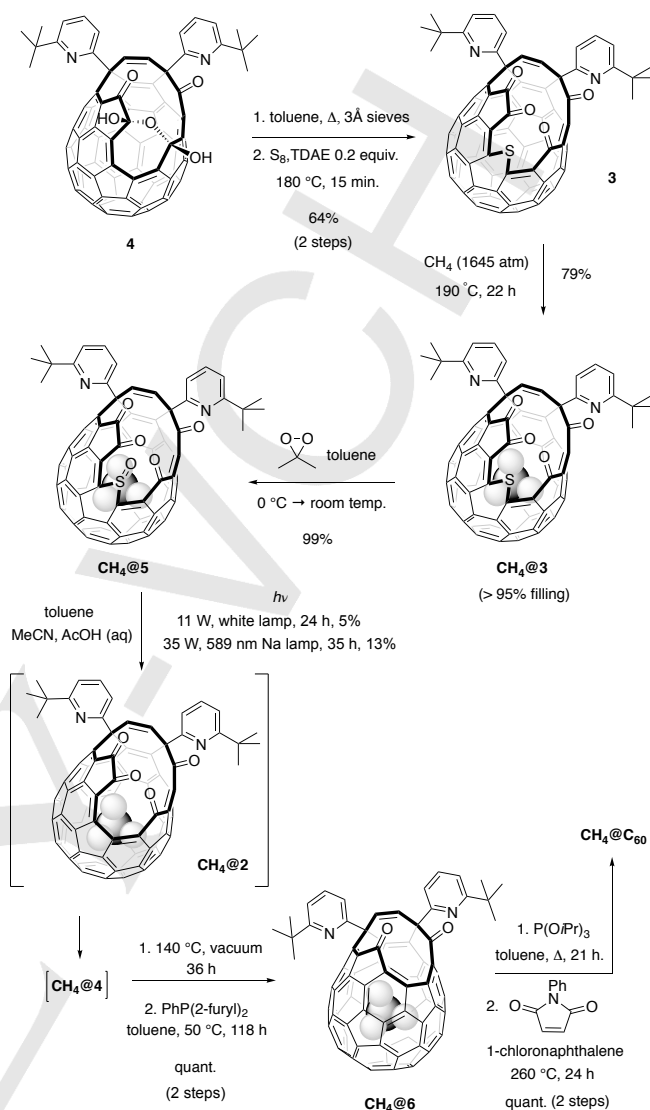
Supporting information for this article is given via a link at the end of the document

COMMUNICATION

exhibited by methane, which exists as three nuclear spin isomers with the $J = 0$ rotational state having nuclear spin $I = 2$, the $J = 1$ rotational state having nuclear spin $I = 1$, and the $J = 2$ rotational state having nuclear spin states $I = 0$ and $I = 1$.^[34,35] Methane is one of the largest possible guests for C_{60} ^[36] and herein, we report conditions for optimised CH_4 encapsulation by **3** and the first successful closure sequence to reform the pristine C_{60} cage. Our work constitutes the first synthesis of $CH_4@C_{60}$ and raises the exciting prospect of access to other endohedral fullerenes, $A@C_{60}$, in which the endohedral species is a 'large' guest molecule; including $A = O_2, N_2, CO, NO, NH_3, CH_3OH, CH_2O$ and CO_2 , as well as the atoms Ar and Kr.

$CH_4@C_{60}$ was prepared according to the procedures shown in Scheme 1. Open-cage fullerene **3** was obtained from bis(hemiketal) **4**^[15] according to the published method.^[25] We have previously shown the 17-membered orifice of **3** to be suitable for entry of a single molecule of methane, achieving 65% encapsulation by heating **3** at 200 °C under 153 atm of methane.^[28] Upon increasing the pressure of methane above 1500 atm, we now obtained $CH_4@3$ with > 95% encapsulation of methane (estimated from the 1H NMR spectrum) after 22 h at 190 °C. Oxidation with dimethyldioxirane^[37] gave the sulfoxide $CH_4@5$ cleanly. Photochemical removal of the sulfinyl group (SO) has been reported for ring-contraction of the sulfoxide derivative of open-cage fullerene **1**, using visible light irradiation.^[13,38-40] Unfortunately, Murata and co-workers found that the sulfoxide derivative of **3** (*i.e.* **5**) does not undergo simple loss of SO under the same conditions, but undergoes decomposition accompanied by a low-yielding rearrangement to a lactone side product.^[41] However, we noted that the dominant species in the positive ion atmospheric pressure photoionisation (APPI) mass spectrum of **5** appears at $m/z = 1102.18$ and corresponds to the radical cation $C_{82}H_{26}N_2O_4^{+ \cdot}$ resulting from loss of SO from **5**, indicating that ring-contraction by photochemical removal of SO is feasible. Since we found that the expected product **2** from the photochemical ring-contraction is unstable under visible light irradiation, we considered that the reaction might be facilitated if **2** could be trapped *in situ* as the bis(hemiketal) **4**. We were pleased to observe that in a mixed solvent system of toluene, acetonitrile and acetic acid (10% v/v aq.), irradiation of sulfoxide **5** (containing endohedral water under the partly aqueous reaction conditions), in the visible range for 24 h with an 11 W bulb, gave a mixture of **4** and $H_2O@4$ in 25% isolated yield with a similar amount of unreacted **5** remaining. A longer period of irradiation did not lead to a higher yield of **4**. Product(s) of polymerisation or decomposition, which were not identified, accounted for the remaining material, and none of the lactone product recovered by Murata *et al.* was isolated.

When $CH_4@5$ was subjected to identical photochemical conditions, the corresponding product of SO loss followed by hydration, $CH_4@4$, was obtained in only 5% yield, retaining >95% methane filling. We confirmed that the observed drop in yield is due to the presence of endohedral methane by carrying out photolysis on a sample of $CH_4@5$ with 83% filling (supporting information section S5), from which the product $CH_4@4$ was obtained with only 57% filling as a result of the much higher-yielding conversion of the portion of the material which does not contain methane.



Scheme 1. Synthesis of $CH_4@C_{60}$. Optimised CH_4 encapsulation by **3** and a successful closure sequence involving photochemical desulfinylation, are applied to the first synthesis of $CH_4@C_{60}$.

The yield of the photochemical ring-contraction was significantly increased upon switching to irradiation with monochromatic (yellow) light at 589 nm, using a low-pressure sodium lamp. A mixture of **5** and $H_2O@5$ was converted to the bis(hemiketal) mixture (**4** + $H_2O@4$) in 43% isolated yield. The corresponding reaction of $CH_4@5$ under irradiation at 589 nm gave $CH_4@4$ in a yield of 13%, in accordance with the expected inhibition of the reaction by endohedral methane, and is a valuable improvement in comparison with the very low yield obtained using white light. It is rare for endohedral species' to affect the reactivity of the fullerene cage,^[42,43] particularly in such a dramatic (and unfortunate) fashion, but while it is disappointing that this step remains low-yielding, with $CH_4@4$ in hand we were now able to adapt known procedures for suturing of the bis(hemiketal) orifice to an intact C_{60} shell.

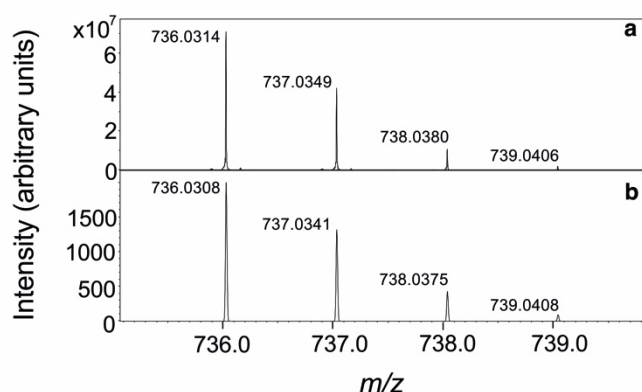


Figure 2. Positive ion APPI mass spectrum of $\text{CH}_4@C_{60}$. (a) Experimental data and (b) model isotope pattern for $C_{61}H_4$; m/z 735–740.

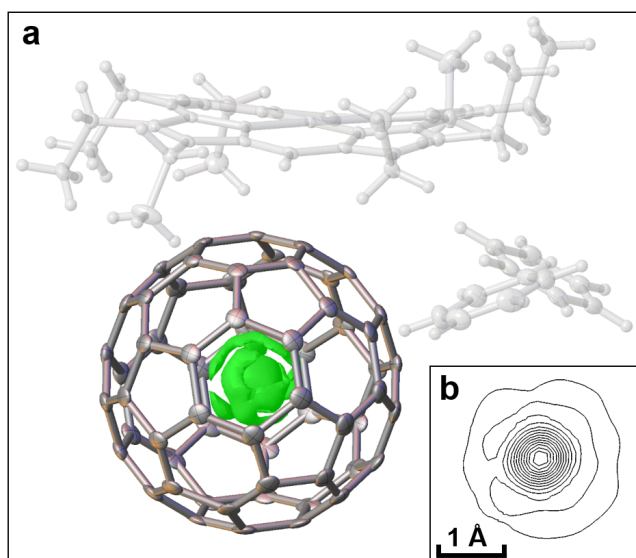


Figure 3. Crystal structure for the nickel(II) octaethylporphyrin / benzene solvate of $\text{CH}_4@C_{60}$. (a) Thermal ellipsoids for the cage atoms of $\text{CH}_4@C_{60}$ and the difference electron density map for endohedral CH_4 (surface drawn at the $0.6 \text{ e}\text{\AA}^3$ level) are shown. Ni(II)OEP and benzene are shown as thermal ellipsoids in white and all thermal ellipsoids are shown at 50% probability. (b) Selected slice through the centre of difference electron density at the CH_4 position, contours drawn at approximately $0.9 \text{ e}\text{\AA}^3$. A faint shell of electron density at a radius of 1.03 \AA from the centre of the cage is visible. This corresponds to the delocalised wavefunction of the methane hydrogen atoms. CCDC 1858399 contains the crystallographic data for this paper and structure details are reported in the supporting information (section S6). The data can be obtained free of charge from The Cambridge Crystallographic Data Centre via <http://www.ccdc.cam.ac.uk/structures>.

$\text{CH}_4@4$ (>95% filling) was contaminated by a trace of $\text{H}_2\text{O}@4$, identified by the ^1H NMR resonance of endohedral water at $\delta = -9.84 \text{ ppm}^{[16]}$ and distinct from the ^1H resonance for endohedral methane in $\text{CH}_4@4$ which appears as a sharp singlet at $\delta = -11.22 \text{ ppm}$ (CDCl_3). Since the percentage filling of H_2O will be amplified by a factor of approx. 5 during photochemical ring

contraction (supporting information section S5.1), we extrapolate the methane filling in $\text{CH}_4@5$ to be >99.5%. In order to avoid final contamination of $\text{CH}_4@C_{60}$ by $\text{H}_2\text{O}@C_{60}$, $\text{CH}_4@4$ was heated at 140°C under a dynamic vacuum ($\sim 0.5 \text{ mm Hg}$) for 36 h to obtain $\text{CH}_4@2$ with accompanying removal of the endohedral water contaminant. No loss of CH_4 was observed. Subsequent reduction to $\text{CH}_4@6$ using di-(2-furyl)phenylphosphine in toluene, at a temperature of 50°C (too low for water re-entry), gave $\text{CH}_4@6$ (>95% filling) in quantitative yield. Endohedral methane appears as a singlet with a shift of $\delta_{\text{H}} = -9.82 \text{ ppm}$ (700 MHz, THF-d_8 , 295 K) in the ^1H NMR spectrum of $\text{CH}_4@6$, and no $\text{H}_2\text{O}@6$ was present. Finally, the orifice of $\text{CH}_4@6$ was sutured, using identical conditions to those reported for $\text{H}_2\text{O}@6$,^[16] and $\text{CH}_4@C_{60}$ was obtained with $100.0 \pm 0.3 \%$ filling after removal of traces of (empty) C_{60} by preparative HPLC on a Cosmosil™ Buckyprep column. An independently prepared sample of $\text{H}_2\text{O}@C_{60}$ was found to co-elute with $\text{CH}_4@C_{60}$, confirming the necessity for removal of contaminant endohedral water earlier in the synthesis.

The positive ion atmospheric pressure photoionisation (APPI) mass spectrum of $\text{CH}_4@C_{60}$ is in agreement with the calculated isotope distribution pattern for $C_{61}H_4$ (Figure 2), and the ultrahigh resolution also confirms that $\text{H}_2\text{O}@C_{60}$ is not present since the isotope patterns for $\text{CH}_4@C_{60}$ and $\text{H}_2\text{O}@C_{60}$ were shown to be non-overlapping (supporting information section S4).

A crystal structure of the nickel(II) octaethylporphyrin / benzene solvate^[44] of $\text{CH}_4@C_{60}$ was obtained (CCDC 1858399) and is similar to that reported for the equivalent C_{60} solvate^[45] with the exception of a spherically symmetrical electron density distribution located at the centre of the fullerene, corresponding to the endohedral methane molecule. The electron density map shows a faint spherical shell around the main centre of the endohedral electron density, at a radius of 1.03 \AA (Figure 3). This shell of distributed electron density corresponds to the delocalised nuclear wavefunction of the methane hydrogens, as expected for a quantum description of the freely rotating molecule. This quantum description is well-established for the analogous systems $\text{H}_2@C_{60}$, $\text{H}_2\text{O}@C_{60}$, and $\text{HF}@C_{60}$, which have been extensively studied by neutron-scattering and infrared spectroscopy.^[17,20–22] A classical description in which the methane explores a random set of orientations would give a similar result. There is no geometrical evidence (within 3-sigma) for distortion of the cage relative to the C_{60} analogue, or displacement of the methane from its centre.

Detailed NMR characterisation of $\text{CH}_4@C_{60}$ was carried out. The ^1H NMR spectrum in 1,2-dichlorobenzene- d_4 displays a singlet at $\delta_{\text{H}} = -5.71 \text{ ppm}$, where the shift results from the shielding effect of the C_{60} cage, compared with $^{12}\text{CH}_4$ in the gas phase which has a chemical shift of $\delta_{\text{H}} = 2.166 \pm 0.002 \text{ ppm}$.^[46] From the natural abundance $^{13}\text{CH}_4@C_{60}$, the measured coupling is $^1J_{\text{HC}} = 124.3 \pm 0.2 \text{ Hz}$ (at 295 K), in comparison with $^1J_{\text{HC}} = 125.3 \text{ Hz}$ (at 292 K) measured in the gas phase.^[47] The liquid state $^{13}\text{C}\{^1\text{H}\}$ NMR spectrum reports a sharp singlet for endohedral methane at $\delta_{\text{C}} = -13.63 \text{ ppm}$ in 1,2-dichlorobenzene- d_4 , again shielded in comparison with the reported shift of $\delta_{\text{C}} = -8.648 \pm 0.001 \text{ ppm}$ measured in the gas phase^[46] (Figure 4a-b).

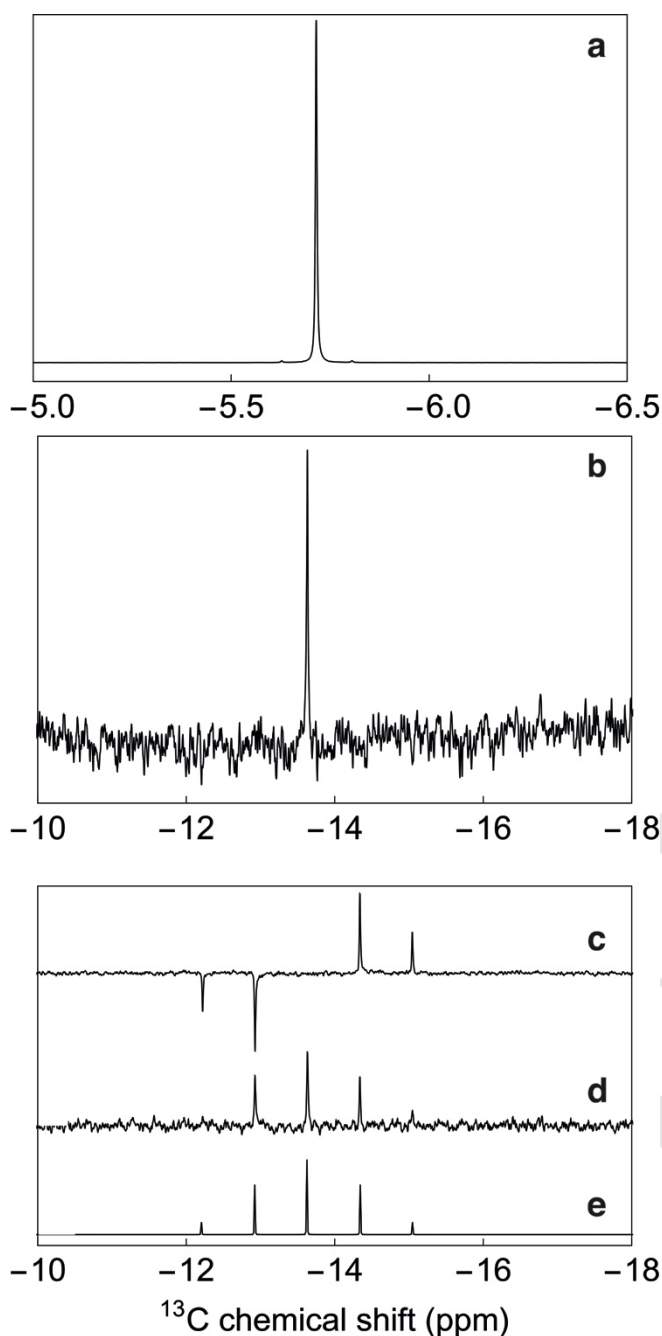


Figure 4. ^1H and ^{13}C NMR resonances for endohedral methane in $\text{CH}_4@C_{60}$. (a) Experimental ^1H NMR resonance of $\text{CH}_4@C_{60}$ acquired with 1 transient, (b) Experimental ^{13}C NMR resonance of $\text{CH}_4@C_{60}$ with ^1H WALTZ16 decoupling (nutration frequency = 14.2 kHz), acquired with 4928 transients and a delay of 10 s between scans, (c) Experimental non-proton-decoupled ^{13}C INEPT spectrum, acquired with 35840 transients and a delay of 4.5 s between scans, (d) Experimental non-proton-decoupled ^{13}C NMR spectrum excited by a single 90° pulse, acquired with 35840 transients and a delay of 4.5 s between scans, (e) Numerical simulation of (d) using *SpinDynamica*.^[50] All experimental spectra were acquired for a degassed 4.5 mM sample of $\text{CH}_4@C_{60}$ in 1,2-dichlorobenzene- d_4 at 16.45 T (^1H nuclear Larmor frequency = 700 MHz and ^{13}C nuclear Larmor frequency = 176 MHz) and 295 K.

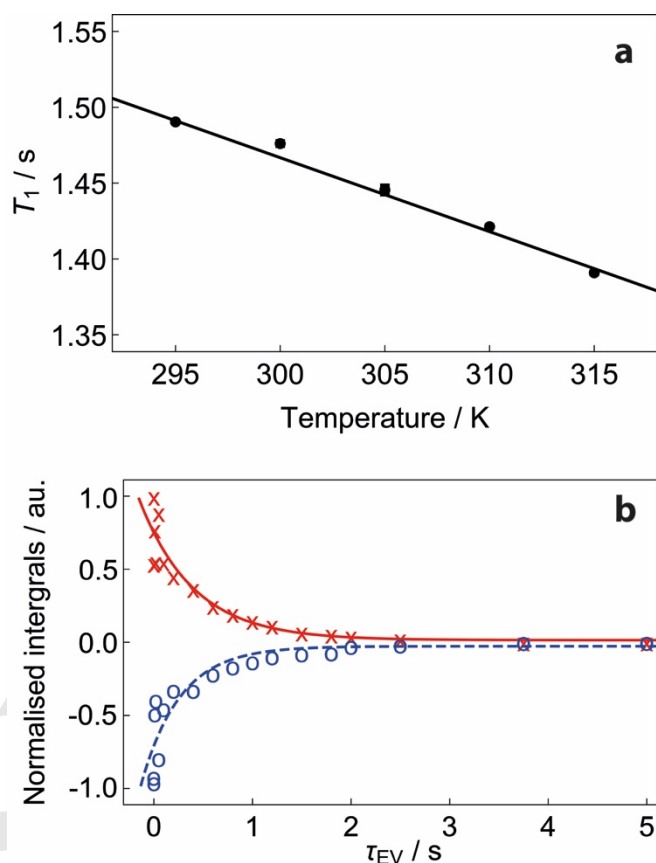


Figure 5. Experimental ^1H and ^{13}C spin-lattice relaxation times for endohedral methane in $\text{CH}_4@C_{60}$. (a) Experimental ^1H spin lattice relaxation as a function of temperature for $^{12}\text{CH}_4@C_{60}$. The best straight line fit to the experimental data points is shown. ^1H longitudinal relaxation times were measured using the inversion-recovery pulse sequence, (b) Experimental ^{13}C spin-lattice relaxation curves for $^{13}\text{CH}_4@C_{60}$ (natural abundance). Spectra were acquired for a degassed 4.5 mM solution of $\text{CH}_4@C_{60}$ in 1,2-dichlorobenzene- d_4 at 16.45 T (^1H nuclear Larmor frequency = 700 MHz) and 295 K. Red data points \times correspond to the satellite at $\delta = -5.638$ ppm; Blue data points \circ correspond to the satellite at $\delta = -5.815$ ppm. The ^{13}C longitudinal relaxation time T_1 was measured using the pulse sequence described in supporting information section S3.2. All signal amplitudes were normalized to the maximum integral (second data point, $\tau_{\text{EV}} = 1$ ms). The fitted curves have single exponential form.

Figure 4c-d shows the relevant section of the INEPT NMR spectrum of $^{13}\text{CH}_4@C_{60}$, alongside experimental and simulated proton-coupled ^{13}C NMR spectra. The INEPT pulse sequence was used as defined by Morris and Freeman^[48] with an interpulse delay of $\tau = \frac{1}{4 J_{\text{HC}}} = 2.012$ ms ($J_{\text{HC}} = 124.3$ Hz). The experimental ^{13}C resonance is a 1:4:6:4:1 quintet with chemical shift $\delta_{\text{C}} = -13.63$ ppm. The ^{13}C NMR resonance for the cage in $\text{CH}_4@C_{60}$ appears at $\delta_{\text{C}} = 143.20$ ppm, shifted by $\Delta\delta = +0.52$ ppm relative to C_{60} itself. This is a large deshielded shift of the cage ^{13}C NMR resonance in comparison with the effect of smaller molecular endohedral species ($\text{HF}@C_{60}$, $\Delta\delta = +0.04$ ppm,^[17] $\text{H}_2@C_{60}$, $\Delta\delta = +0.08$ ppm^[16] and $\text{H}_2\text{O}@C_{60}$, $\Delta\delta = +0.11$ ppm^[15,16]) consistent with the large size of methane. Correlation of $\Delta\delta$ with the van der Waals radius of the enclosed species has been described for the inert gas@ C_{60} series.^[49]

The ^1H spin-lattice relaxation time constant of $^{12}\text{CH}_4@C_{60}$ was found to be $T_1 = 1.4904 \pm 0.0005$ s at 295 K. Measurement of T_1 as a function of temperature indicates a clear increase in relaxation rate constant (T_1^{-1}) with increasing temperature. This is indicative of a significant spin-rotation contribution to the relaxation, and is consistent with ^1H relaxation of methane in the gas phase^[51] (Figure 5a).

The ^{13}C T_1 values for endohedral methane, reported by the ^{13}C satellites of the ^1H spectrum using a modified INEPT sequence (supporting information section S3.2), are slightly different: $T_1 = 0.39 \pm 0.14$ s for the less shielded satellite, and $T_1 = 0.55 \pm 0.14$ s for the more shielded satellite (Figure 5b). This difference is likely to be associated with cross-correlated relaxation effects.^[52]

In summary, $\text{CH}_4@C_{60}$, the first example of an organic molecule trapped in C_{60} , has been synthesised. CH_4 is the largest molecule, with the greatest number of atoms, to have been encapsulated in C_{60} to date. The first step of the orifice contraction was strongly inhibited by the presence of endohedral methane, resulting in a low yield for the key photolytic step. $\text{CH}_4@C_{60}$ was characterised by high resolution mass spectrometry, NMR spectroscopy and X-ray crystallography. ^1H spin-lattice relaxation times for endohedral methane are similar to those observed in the gas phase, providing evidence that methane is freely rotating inside the C_{60} cage. The experimental ^{13}C NMR chemical shift of the cage carbon is shifted by +0.52 ppm relative to empty C_{60} . We find no evidence for distortion of the cage from a crystal structure of the nickel(II) octaethylporphyrin / benzene solvate of $\text{CH}_4@C_{60}$. In the crystal structure, the hydrogen atoms of methane appear as a spherically symmetric sphere of electron density consistent with a delocalised quantum state. Neutron scattering, infrared spectroscopy and cryogenic NMR experiments are now planned in order to study spin-isomerism and spin-isomer conversion of the encapsulated methane molecules. The successful synthesis of $\text{CH}_4@C_{60}$ opens a route to novel endofullerenes $A@C_{60}$ enclosing 'large' endohedral species A, such as $A = \text{O}_2$, NO , NH_3 , N_2 , CO_2 , CH_3OH and H_2CO , with exciting prospects for the study of these encapsulated small molecules.

Acknowledgements

This work was supported by the Engineering and Physical Sciences Research Council (EP/M001962/1, EP/P009980/1), including core capability (EP/K039466); and the European Research Council (786707-FunMagResBeacons).

Keywords: endohedral fullerene • mass spectrometry • NMR spectroscopy • synthetic methods • X-ray diffraction

- [1] H. W. Kroto, J. R. Heath, S. C. O'Brien, R. F. Curl, R. E. Smalley, *Nature* **1985**, *318*, 162-163.
- [2] J. R. Heath, S. C. O'Brien, Q. Zhang, Y. Liu, R. F. Curl, H. W. Kroto, F. K. Tittel, R. E. Smalley, *J. Am. Chem. Soc.* **1985**, *107*, 7779-7780.
- [3] X. Lu, L. Feng, T. Akasaka, S. Nagase, *Chem. Soc. Rev.* **2012**, *41*, 7723-7760.
- [4] A. A. Popov, *Nanostruct. Sci. Technol.*, **2017**, 1-34.
- [5] A. A. Popov, S. F. Yang, L. Dunsch, *Chem. Rev.* **2013**, *113*, 5989-6113.
- [6] S. Osuna, M. Swart, M. Sola, *Chem. - Eur. J.* **2009**, *15*, 13111-13123.
- [7] M. Saunders, R. J. Cross, H. A. Jiménez-Vázquez, R. Shimshi, A. Khong, *Science* **1996**, *271*, 1693-1697.
- [8] T. A. Murphy, T. Pawlik, A. Weidinger, M. Hohne, R. Alcalá, J. M. Spaeth, *Phys. Rev. Lett.* **1996**, *77*, 1075-1078.
- [9] S. C. Chuang, F. R. Clemente, S. I. Khan, K. N. Houk, Y. Rubin, *Org. Lett.* **2006**, *8*, 4525-4528.
- [10] Y. Rubin, *Chem. - Eur. J.* **1997**, *3*, 1009-1016.
- [11] Y. Rubin, T. Jarrosson, G. W. Wang, M. D. Bartberger, K. N. Houk, G. Schick, M. Saunders, R. J. Cross, *Angew. Chem., Int. Ed. Engl.*, **2001**, *40*, 1543-1546.
- [12] G. Schick, T. Jarrosson, Y. Rubin, *Angew. Chem., Int. Ed. Engl.* **1999**, *38*, 2360-2363.
- [13] K. Komatsu, M. Murata, Y. Murata, *Science* **2005**, *307*, 238-240.
- [14] Y. Murata, M. Murata, K. Komatsu, *J. Am. Chem. Soc.* **2003**, *125*, 7152-7153.
- [15] K. Kurotobi, Y. Murata, *Science* **2011**, *333*, 613-616.
- [16] A. Krachmalnicoff, M. H. Levitt, R. J. Whitby, *Chem. Commun.* **2014**, *50*, 13037-13040.
- [17] A. Krachmalnicoff *et al*, *Nat. Chem.* **2016**, *8*, 953-957.
- [18] A. Krachmalnicoff, R. Bounds, S. Mamone, M. H. Levitt, M. Carravetta, R. J. Whitby, *Chem. Commun.* **2015**, *51*, 4993-4996.
- [19] M. H. Levitt, *Philos. Trans. R. Soc., A* **2013**, *371*, 20120429.
- [20] C. Beduz *et al*, *Proc. Natl. Acad. Sci. USA* **2012**, *109*, 12894-12898.
- [21] S. Mamone *et al*, *J. Chem. Phys.* **2009**, *130*, 081103.
- [22] S. Mamone, M. Jiménez-Ruiz, M. R. Johnson, S. Rols, A. J. Horsewill, *Phys. Chem. Chem. Phys.* **2016**, *18*, 29369-29380.
- [23] M. Z. Xu, F. Sebastianelli, B. R. Gibbons, Z. Bacic, R. Lawler, N. J. Turro, *J. Chem. Phys.* **2009**, *130*, 224306.
- [24] B. Meier, S. Mamone, M. Concistrè, J. Alonso-Valdesueiro, A. Krachmalnicoff, R. J. Whitby, *Nat. Commun.* **2015**, *6*, 8112.
- [25] T. Futagoishi, M. Murata, A. Wakamiya, T. Sasamori, Y. Murata, *Org. Lett.* **2013**, *15*, 2750-2753.
- [26] T. Futagoishi, M. Murata, A. Wakamiya, Y. Murata, *Angew. Chem. Int. Ed. Engl.* **2015**, *54*, 14791-14794.
- [27] T. Futagoishi, M. Murata, A. Wakamiya, Y. Murata, *Angew. Chem. Int. Ed. Engl.* **2017**, *56*, 2758-2762.
- [28] S. Bloodworth *et al*, *Chemphyschem* **2018**, *19*, 266-276.
- [29] S. Hasegawa, Y. Hashikawa, T. Kato, Y. Murata, *Angew. Chem. Int. Ed. Engl.* **2018**, *57*, 12804-12808.
- [30] T. Futagoishi, T. Aharen, T. Kato, A. Kato, T. Ihara, T. Tada, M. Murata, A. Wakamiya, H. Kageyama, Y. Kanemitsu, Y. Murata, *Angew. Chem. Int. Ed. Engl.* **2017**, *56*, 4261-4265.
- [31] S. Mamone *et al*, *J. Chem. Phys.* **2014**, *140*, 194306.
- [32] B. Meier, K. Kouřil, C. Bengs, H. Kouřilova, T. C. Barker, S. J. Elliott, S. Alom, R. J. Whitby, M. H. Levitt, *Phys. Rev. Lett.* **2018**, *120*, 266001.
- [33] N. J. Turro, A. A. Martí, J. Y.-C. Chen, S. Jockusch, R. G. Lawler, M. Ruzzi, E. Sartori, S. C. Chuang, K. Komatsu, Y. Murata, *J. Am. Chem. Soc.* **2008**, *130*, 10506-10507.
- [34] P. Cacciani, J. Cosleou, M. Khelkhal, P. Cermak, C. Puzzarini, *J. Phys. Chem. A* **2016**, *120*, 173-182.
- [35] T. Sugimoto, K. Yamakawa, I. Arakawa, *J. Chem. Phys.* **2015**, *143*, 224305.
- [36] K. E. Whitener, R. J. Cross, M. Saunders, S. Iwamatsu, S. Murata, N. Mizorogi, S. Nagase, *J. Am. Chem. Soc.* **2009**, *131*, 6338-6339.
- [37] W. Adam, J. Bialas, L. Hadjirapoglou, *Chem. Ber.* **1991**, *124*, 2377-2377.
- [38] Y. Morinaka, F. Tanabe, M. Murata, Y. Murata, K. Komatsu, *Chem. Commun.* **2010**, *46*, 4532-4534.
- [39] M. Murata, S. Maeda, Y. Morinaka, Y. Murata, K. Komatsu, *J. Am. Chem. Soc.* **2008**, *130*, 15800-15801.
- [40] M. Murata, Y. Murata, K. Komatsu, *J. Am. Chem. Soc.* **2006**, *128*, 8024-8033.
- [41] T. Futagoishi, M. Murata, A. Wakamiya, Y. Murata, *Chem. Commun.* **2017**, *53*, 1712-1714.

- [42] E. E. Maroto, J. Mateos, M. García-Borràs, S. Osuna, S. Filippone, M. A. Herranz, Y. Murata, M. Solà, N. Martín, *J. Am. Chem. Soc.* **2015**, *137*, 1190-1197.
- [43] S. Vidal, M. Izquierdo, S. Alom, M. García-Borràs, S. Filippone, S. Osuna, M. Solà, R. J. Whitby, N. Martín, *Chem. Commun.* **2017**, *53*, 10993-10996.
- [44] M. M. Olmstead, D. A. Costa, K. Maitra, B. C. Noll, S. L. Phillips, P. M. van Calcar, A. L. Balch, *J. Am. Chem. Soc.* **1999**, *121*, 7090-7097.
- [45] H. M. Lee, M. M. Olmstead, T. Suetsuna, H. Shimotani, N. Dragoe, R. J. Cross, K. Kitazawa, A. L. Balch, *Chem Commun*, **2002**, 1352-1353.
- [46] A. Antušek, K. Jackowski, M. Jaszuński, W. Makulski, M. Wilczek, *Chem. Phys. Lett.* **2005**, *411*, 111-116.
- [47] B. Bennett, W. T. Raynes, *Mol. Phys.* **1987**, *61*, 1423-1430.
- [48] G. A. Morris, R. Freeman, *J. Am. Chem. Soc.* **1979**, *101*, 760-762.
- [49] R. G. Lawler, *Nanostruct. Sci. Techn.* **2017**, 229-263.
- [50] C. Bengs, M. H. Levitt, *Magn. Reson. Chem.* **2018**, *56*, 374-414.
- [51] C. J. Jameson, A. K. Jameson, N. C. Smith, J. K. Hwang, T. N. Zia, *J. Phys. Chem.* **1991**, *95*, 1092-1098.
- [52] A. Kumar, R. C. R. Grace, P. K. Madhu, *Prog. Nucl. Magon. Res. Spectrosc.* **2000**, *37*, 191-319.
-

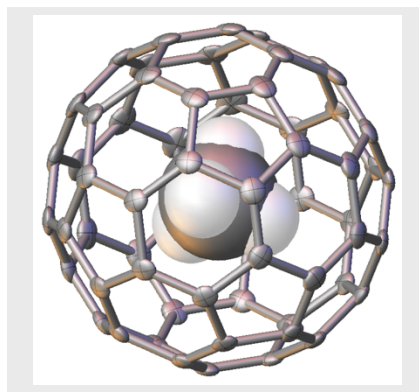
COMMUNICATION

Entry for the Table of Contents (Please choose one layout)

Layout 1:

COMMUNICATION

The endohedral fullerene $\text{CH}_4@C_{60}$ has been synthesised for the first time using photochemical desulfinylation of an open fullerene as the key step. Methane is a much larger molecule than has been previously encapsulated in the closed C_{60} cage and is amongst the largest of possible guests.



*Sally Bloodworth, Gabriela Sotinova, Shamim Alom, Sara Vidal, George R. Bacanu, Stuart J. Elliott, Mark E. Light, Julie M. Herniman, G. John Langley, Malcolm H. Levitt, and Richard J. Whitby**

Page No. – Page No.

First synthesis and characterisation of $\text{CH}_4@C_{60}$

Layout 2:

COMMUNICATION

((Insert TOC Graphic here))

*Author(s), Corresponding Author(s)**

Page No. – Page No.

Title

Text for Table of Contents
